

# Mining the modular structure of protein interaction networks at different resolution levels

Berenstein A.<sup>1</sup>✉, Piñero J.<sup>2</sup>✉, Furlong L.I.<sup>2</sup>, Chernomoretz A.<sup>1,3\*</sup>

<sup>1</sup>Depto de Física, FCEyN, UBA and IFIBA, CONICET, Pabellón 1, Ciudad Universitaria, 1428 Buenos Aires, Argentina

<sup>2</sup> Research Programme on Biomedical Informatics (GRIB), Hospital del Mar Medical Research Institute (IMIM), Universitat Pompeu Fabra (UPF), C/Dr. Aiguader, 88, 08003 – Barcelona, Spain

<sup>3</sup>Laboratorio de Biología de Sistemas Integrativa, Fundación Instituto Leloir, Buenos Aires, Argentina

Cluster-based descriptions of biological networks have received much attention in recent years, fostered by accumulated evidence of the existence of meaningful correlations between topological network clusters and biological functional modules. Several well-performing clustering algorithms exist to infer topological network partitions. However, due to respective technical ‘idiosyncrasies’, they might produce modular descriptions that provide network pictures at different resolution levels. We aimed to analyze how these alternative modular descriptions could condition the outcome of follow-up network biology analysis.

We considered a human protein interaction network and two paradigmatic cluster recognition algorithms, namely: the Clauset-Newman-Moore and the *infomap* procedures. We analyzed at what extent both procedures yielded different results in terms of cluster sizes, their biological congruency and displayed meso-scale connectivity patterns. We specifically studied the case of aging related proteins, and showed that only the high-resolution modular description, achieved by *infomap*, could unveil statistically significant associations between them and inter/intra modular connectivity schemes. In particular, we found that aging related proteins were more likely to reside in the interface of network modules, possibly linking distinct biological processes. Besides reporting novel biological insights that could be gained from the discovered associations, our results warns against possible technical concerns that might affect the tools used to mine for interaction patterns in network biology studies.

## 1 INTRODUCTION

One of the major challenges of systems biology is the understanding of the cellular and molecular basis of high-level biological functionality and complex phenotypes. A promising approach to address these problems relies on the characterization of cellular functionality in terms of global descriptions of the interwoven set of intracellular biochemical reactions as recapitulated by complex network methodologies [1,2]. In this context modular and cluster-based representations of biological networks help to establish and take advantage of meaningful correlations between topological network clusters (which are formed from nodes which are more densely connected with each other than with their neighborhood), and Hartwell’s original idea of “biological functional modules”, defined as a group of cellular molecular components and their interactions that carry out a specific biological function [3, 4,5].

A particularly insightful use of network’s modular descriptions to unveil their organization was introduced by Guimera and Amaral [6–8]. They proposed to classify network nodes according to their intra and inter-module connectivity patterns into seven different universal roles [6]. To that end, they introduced two observables: the intra-cluster connectivity,  $Z$ , and the participation coefficient,  $P$  of a node. While the first parameter describes the degree of a node compared to the degree of nodes that belong to the same community, the second one quantifies to what extent a node connects to different modules. In this way they were able to depict highly informative ‘cartographic representations’ of several metabolic networks. Furthermore, they showed that non-hub high-participation nodes, detected

in *E.coli* metabolic network, tend to display unusually low evolutionary rates, suggesting that relevant biology could indeed be underpinned with the proposed methodology [7].

Being a module-based scheme, an appealing factor of Guimera's analysis is that it does not rely neither on strictly local (i.e. features involving only properties of a node and its direct neighbors) nor global network features, but rather on connectivity patterns displayed at the meso-scale level. In fact, the very notion of network community is used in order to set the meaningful scale over which the connectivity analysis is performed. Noticeably, the identification of network modules or communities is in fact a mathematically ill-posed problem, in the sense that there is no such a thing as an *a-priori* objective and hypothesis-free definition of how clusters should be defined. In this way, the concept of network *clusters* (or *communities*) entails - often implicitly - the assumption of precise notions of connectivity and scale resolution levels employed to map local heterogeneities into cluster aggregates. In practice, this results in the co-existence of many different community recognition procedures that might produce different network partitions (see [9] for an extensive review). Moreover, it renders the question of how these methodologies would perform in terms of their ability to unveil biologically significant patterns.

In the present contribution we study the implications that eventual discrepancies in modular resolution levels could produce in follow-up biological analysis. We concentrated our work on two important aspects of the problem. On one hand we identified network community partitions at different resolution levels (as obtained by different cluster recognition algorithms) and analyzed them in terms of their biological homogeneity. On the other hand, we characterized network meso-scale connectivity features taking into account Guimera's cartographic role description. Finally we illustrate for a particular example involving aging-related gene products, how the different resolution level, displayed by the network modular descriptions, condition the ability of the considered clustering methodologies to mine for significant connections between specific intra/inter modular connectivity patterns and complex phenotypes.

In order to analyze the modular structure of a given protein interaction network at different resolution levels, we considered two paradigmatic network community detection procedures: the Clauset-Newman-Moore (CNM) methodology [10], and the infomap algorithm [11]. These well-known methodologies make use of qualitatively different optimization criteria. In particular, the first one is part of a wide-spread used family of community detection procedures that are based on the optimization of a figure-of-merit known as network modularity. Noticeably, in 2007, Fortunato & Barthelemy demonstrated that a theoretical resolution limit exists for this kind of algorithms that leads to the systematic merge of small clusters in larger modules, even when the clusters are well defined and loosely connected to each other [12]. Since then, many contributions, mainly inside the physics community, further explored this effect, proposed alternative methodologies, and established comparative studies considering ad-hoc benchmark network models [13–16]. However, to the best of our knowledge, this effect has not been evaluated in the context of biological networks.

The infomap algorithm, on the other hand, relies on very different optimization criteria [11]. Clusters are defined in order to minimize the average description length of a random walk process taking place over the graph. This procedure was found to be not affected by this resolution limit effect when benchmark networks were considered [15].

Despite these developments, modularity maximization is still one of the most popular techniques for the detection of community structure in graphs. In particular, we found that in consonance with the modularity-based community detection procedure employed by Guimera in its original series of papers, many recent cluster-based analysis of different biological problems [17–19], were tackled considering slight variations of the same kind of modularity maximization guided algorithms. In this context, the comparison presented in this work will also serve to illustrate and put a word of caution about how the “idiosyncrasy” of the considered algorithms could impact on follow-up biological analysis of real protein interaction datasets.

## 2 MATERIAL AND METHODS

We considered the set of protein interactions recapitulated in HIPPIE, an integrated protein interaction network with experiment based quality scores [20]. The high-confidence version of the network (v1.5, downloaded on April 2012) included 31068 interactions among 8277 proteins. We focused our analysis on the giant component of this graph, comprising 8000 nodes and 30835 edges, that we dubbed PIN for future reference. An analysis of several network topological features is included as Supplementary Material (see text ST1 and figure SF1 in Sup. Mat.). In our analysis, we also considered a curated database of genes associated with the human aging phenotype provided by *GenAge* [21]. The downloaded dataset (October 2013) comprised 298 genes, and 261 of them could be mapped to PIN.

### 2.1 Meso-scale network topological features

Two topological features, introduced by Guimera and Amaral, were central to our analysis: the *intra-cluster connectivity*,  $Z$ , and the *participation coefficient*,  $P$  of a node [7].

$$Z_i = \frac{k_i - \overline{k_{C_i}}}{\sigma_{k_{C_i}}}, \quad P_i = 1 - \sum_{c=1}^M \left( \frac{k_{iC}}{k_i} \right)^2$$

where  $k_i$  is the degree of the node- $i$ ,  $\overline{k_{C_i}}$  is the mean degree of nodes in module  $C_i$ ,  $\sigma_{k_{C_i}}$  is the standard deviation of the nodes degree in that cluster,  $k_{iC}$  is the number of connections of node  $i$  to members of cluster  $C$ , and  $M$  is the total number of communities in the network. These quantities can be considered as meso-scale descriptors as they explicitly depend on the network’s modular structure.  $Z_i$  measures how well-connected node- $i$  is with respect to the other nodes in the module. On the other hand, the participation coefficient  $P_i$  is close to 1 if its links are uniformly distributed among all the modules.

### 2.2 Network null models

To explore local and global structural properties of PIN we considered two different network null models: an Erdos-Renyi (ER) [22], and a fully rewired version (RW) of the real network [23]. Both control graphs preserved the number of nodes and edges of the original network. The ER graph had the same link density than the original network but, as edges were assigned randomly, it presented no correlations of any order. On the other hand, the RW model preserved the original degree distribution, but lacked second and higher order correlations that might exist in the real graph. All network-related

calculations were performed using the R statistical framework (v2.15.1) [24] and the igraph library (v0.6-2) [25].

### 2.3 Modular network description

We considered two well-established network community recognition methodologies: the Clauset-Newman-Moore (CNM) modularity optimization algorithm [10], and the *infomap* procedure [11]. A brief description of the optimization criteria at use by each algorithm was included as Supplementary Material (see sup. text ST2). A thorough analysis and performance comparison of both algorithms can be found in [13-15].

### 2.4 Biological homogeneity index (BHI) of network partitions

The BHI figure-of-merit measures the degree a given partition embodies biologically meaningful clusters, using a reference set of functional classes [26]. It basically quantifies whether genes placed in the same cluster belong to the same functional class. In our case, we relayed on biological knowledge embedded in Gene Ontology protein annotations. A brief description of the considered BHI was included in the Supplementary Material ST3.

### 2.5 Degree control for role enrichment estimation

A bootstrapping procedure was devised to control the node's degree distribution confounding factor for the role enrichment analysis. For each enrichment test, we considered an ensemble of 1000 control random gene-sets having the same degree distribution than the genes under study. A p-value level was assigned according to the number of random realizations displaying the same or larger effects (over/under representation significance) than the ones observed in the original data. Each random realization was built blindly selecting genes from pools of given degree levels in order to conform the degree distribution displayed by the original gene set (see Sup Material ST4 for details).

## 3 RESULTS

### 3.1 CNM and infomap mine the PIN modular structure at different resolution levels

The modular organization of the PIN was explored considering the *CNM* and *infomap* procedures. Both methodologies resulted in network partitions displaying similar modularity levels ( $Q_{infomap}=0.52$  and  $Q_{infomap}=0.54$ ). These values were much higher than the ones obtained in an ensemble of 1000 randomly rewired versions of the PIN that preserved the original degree distribution ( $Q_{infomap-rwn}=0.255\pm 0.001$ ,  $Q_{CNM-rwn}=0.313\pm 0.001$ ) stressing the relevance of second and higher order correlations present in the real network in connection with the emergence of the observed modular structure.

Although the partitions found by both algorithms attained similar modularity values, large differences were observed in terms of the corresponding community size distributions. For instance, whereas there were no *infomap* communities exceeding four hundred nodes, the *CNM* partition included four communities with more than a thousand nodes each.

The number of internal links,  $l_{int}$ , of a given cluster was used as a proxy of the cluster size (see Fig S2a) and resulted a relevant magnitude to understand qualitative features of the obtained partitions. Figure 1 displays the cumulative cluster-size distribution function,  $F_{c-size}$ , as a function of  $l_{int}$  values, and allows to visualize how the network nodes were distributed in clusters of increasing  $l_{int}$  levels. For *CNM* structures, an abrupt change in  $F_{c-size}(l_{int})$  takes place for a number of internal links of order  $l_{int} \sim \lambda \equiv \nu L$  (where  $L$  is the number of edges of the network). This qualitative change in  $F_{c-size}$  suggested the existence of a dominant size scale in the obtained modular description, as 90% of the total number of network nodes was found inside the 8 largest detected *CNM* communities displaying  $l_{int} > \lambda$  (red filled circles in Fig 1). Importantly, the observed value for  $\lambda$  agrees with the natural scale that was reported to operate in modularity optimization algorithms as a consequence of the existence of a cluster resolution limit for this kind of optimization procedures[12]. In this respect, Fortunato and collaborators have shown that the optimization of the modularity figure-of-merit leads to the systematic merge of small clusters in larger modules, even when the clusters were well defined and loosely connected to each other [12,15].

On the contrary, for *infomap* clusters (empty squares in Fig 1), there is a smooth increase of  $F_{c-size}$ . This means that the network mass could be split into network sub-structures which spanned a wide range of cluster sizes and did not present any recognizable natural size scale. In this way, the results obtained for the considered PIN agreed with Lancichinetti *et al* general observations: differently from *CNM*, the *infomap* procedure provided a network modular description of multi-resolution character [15].

We also found that *infomap* clusters were virtually included inside *CNM* modules, as almost 90% of *infomap* internal links were also internal links in *CNM* clusters (86% of *infomap* intra-cluster node pairs were preserved in the alternative *CNM* partition), and only 66% of *CNM* internal links were preserved as internal *infomap* links (5% of the total *CNM* intra-cluster pair of nodes were preserved under the *infomap* description). As can be seen from Figure S2b, almost the totality (~99%) of broken *CNM*-internal links took place in the largest *CNM* detected structures, and only 1% in *CNM* clusters of internal-link density values lower than the  $\nu L/2$  level.

Summing-up, all our findings were consistent with a scenario where *infomap* finer structures were merged into larger assemblies under the *CNM* description (graphical examples for this general tendency were reported in figure S3). Both partitions reported in fact reconcilable descriptions of the PIN, but the community structure revealed by *infomap* provided a finer granularity level than the one achieved by the *CNM* procedure.

### 3.2 Network structures identified at high resolution levels present higher biological congruency

We considered the biological homogeneity index, BHI, (see Methods) to investigate to what extent different network structures identified at different resolution levels correlated with external biological evidence. BHI values for the 8 *CNM* largest communities, were depicted as red points in Figure 2 (*CNM* clusters were ordered according to decreasing size). Green triangles show the BHI level of the *infomap* partition of clusters included in the respective *CNM* structure. For each *CNM* community, boxplots depict distributions of BHI values estimated for an ensemble of 1000 random shuffling realizations of the corresponding *infomap* labels. The BHI levels of *infomap* partitions were systematically higher than the ones observed for the corresponding *CNM* ones (Figure 2), suggesting that the higher granularity level

provided by the first algorithm resulted in a significant increase of the overall biological consistency of the detected structures. We could verify that the gain in functional coherence displayed by *infomap* did not come from cluster-size effects alone, as we found for all cases that more than 95% of the random label reassignments presented lower BHI levels than the value displayed by the original *infomap* partition. These findings supported the idea that *infomap* communities represent meaningful graph substructures with higher levels of biological congruence.

### 3.3 Functional cartography at different resolutions

Meso-scale topological features of the PIN nodes were analyzed studying how they were distributed over the Z-P plane when the *CNM* and *infomap* procedures were alternatively considered (see Fig 3). Dashed lines in the figure delineate regions corresponding to the seven different universal roles introduced by Guimera [6]. It can be appreciated from both panels, that points were not homogeneously distributed in the plane, but they scattered around three local high-density regions laying on the: ultra-peripheral ( $Z \sim -0.5, P \sim 0$ ), peripheral ( $Z \sim -0.5, P \sim 0.5$ ), and connector ( $Z \sim -0.5, P \sim 0.65$ ) areas. Moreover, the coarser resolution level achieved with the *CNM* algorithm resulted in a general tendency to assign lower participation coefficient values to network nodes (a more detailed quantification of this effect is provided in Sup Table 1).

This last observation is consistent with the fact that the *CNM* community detection procedure resulted in larger community structures and consequently presented less intra-cluster surfaces than the *infomap* methodology. In other words, 'internal' surfaces might appear within large *CNM* clusters when the *infomap* partition was considered (Fig S2b), causing a number of originally intra-*CNM*-cluster links to become edges connecting different *infomap* clusters.

The implications of these discrepancies are not usually addressed in the network biology literature. In fact, several recent studies in different biological contexts, used methodologies based on modularity optimization procedures to characterize PIN nodes in terms of topographic roles [17–19]. For these cases, a low number of high-participation nodes were typically reported. However, we want to stress that this was not an intrinsic network feature. Had the *infomap* clustering procedure been used for the characterization of those networks, a noticeable increase in the number of high participation role nodes would have been observed (see supplementary figure S4 and text ST5).

### 3.4 Meso-scale connectivity patterns of aging-related proteins probed at different resolutions

In this section we aimed to investigate to what extent the resolution of the considered modular description could condition the finding of significant and non-trivial correlations between complex high-level phenotypes and PIN's meso-scale connectivity patterns. We focused our attention in a set of gene products related to aging: the aging related genes (ARG). Aging is a complex process associated to several complex diseases, that is affected by both, environmental and genetic factors [27]. A lot of effort has been devoted to characterize the genetic basis of aging and resulted in the identification of genes that: are able to modulate the aging process (e.g. gene mutants that increase maximum lifespan in model organisms or linked to human longevity) [28], display transcriptional changes that correlate with age [29], or show specific DNA methylation patterns [30]. Integrative network-based

methodologies have already been employed to provide a system-level understanding of aging [28,31,32]. In particular, Xue *et al* have considered a network model of aging integrating a PPI network with gene expression data [31]. They defined network modules analyzing correlation patterns of gene transcriptional profiles and, in the same spirit of the present contribution, found that aging genes were unevenly distributed in their aging-network. Interestingly, they reported that module interfaces - loosely defined as vertices presenting first neighbors located in different modules- had 2-3 fold enrichment in aging associated genes over that the module's cores. In connection with this last finding, we reasoned that the *participation* feature analyzed in the present contribution is particularly well suited to provide a further quantitative topological description of aging-related genes in the context of PIN analysis.

As was already shown in Figure 3 and Table S1, the use of *infomap* gave rise to a noticeable increase in protein vertex *participation* values with respect the *CNM*-based characterization. This effect was particularly evident for ARG nodes. Participation-based ROC curves calculated for ARG genes ( $AUC_{infomap}=0.76$  and  $AUC_{CNM}=0.65$ ) displayed (see Fig S5) statistically significant differences between high and low granularity modular descriptions ( $p_v=2.2 \cdot 10^{-16}$ , deLong's test). This finding suggested that, when estimated at the finer resolution level provided by *infomap* communities, ARG genes were actually boosted toward much higher relative *participation* levels. Therefore, the *participation* feature estimated using *infomap* cluster's definition could better bring out the same tendency reported in [31] regarding aging-related genes to be located at the interfaces of network-communities.

We then explored whether aging-related genes were biased to display specific roles over the network. The results reported in TableS2 (ARG-dataset column) showed that *provincial-hub* and *connector-hub* roles displayed the strongest enrichment in ARG when the *CNM* methodology was adopted. On the other hand *kinless* and *kinless-hub* categories were significantly enriched when *infomap* methodology was considered. Noticeably, under this last analysis alternative, a 64% larger set of ARG were involved in enriched topographic categories and more extreme significance signal levels were achieved, suggesting that the community resolution level provided by *infomap* made a better job highlighting the bias towards high participation roles displayed by ARG genes

We further examined whether similar insight could be gained from the same interaction data considering several topological features other than the *participation* coefficient (e.g. the degree and the betweenness of a node). This point was particularly relevant in our case, as the considered aging-related gene set happened to display rather high *degree* levels over the PIN (see Fig S6), making the node's *degree* a potential confounding factor for our analysis. In order to de-convolve the *degree* signal from *participation* values we performed a bootstrap analysis for the cartographic role enrichment (see Methods). Due to data scarcity of network nodes of high degree levels we considered for this analysis a reduced aging-related gene set (ARG') obtained discarding the top-10% most connected vertices of the original ARG set (see Methods and Sup.Mat Fig S7 for details). Interestingly, we found that only the *infomap-kinless* category enrichment was significant under the bootstrap analysis (see Table S2, ARG'-

dataset column). Hence, these results showed that the high resolution level of the *infomap* community structure allowed highlighting the single non-trivial cartographic role enrichment that could not be explained by the effect of the aging gene-set degree distribution.

Having established the relevance of the granularity of the considered modular network description for the analysis of this protein set, we further wanted to examine whether other network features were also able to provide non-trivial evidence to distinguish aging related genes from the considered protein interaction data. In particular, we analyzed the performance of these indicators in connection with their ability to bring out mid/poorly connected ARG genes, i.e. unimportant and non-central nodes from the point of view of their degree level. We thus focused our attention on a subset of PIN by removing the 10% of genes with highest degree values (i.e. removing from the analysis nodes with  $k > 18$ ), and examined the use of *infomap*-participation to bring out this subset of ARG genes from PIN data. We compared its performance with: the participation feature estimated at a broader resolution (CNM-participation), the node degree, and two alternative measures of a node's information-flow related capabilities: *betweenness* and *bridging* centrality. This last feature quantifies to what extent a node is located between well-connected regions (see [33] for details).

Figure 4 shows ROC curves obtained for the considered features calculated over the analyzed degree-bounded gene-set. Noticeably, along the false-positive-rate (i.e. 1-specificity) range spanned by *infomap*-kinless ARG genes (1-specificity values in the interval  $[0, 0.045]$ ) the *infomap*-participation presented the largest sensitivity among the considered descriptors. In particular, regardless of its absolute performance as a topological predictor, the *infomap*-participation performed better than the CNM-participation feature (i.e. a participation characterization estimated at a broader resolution), and also better than the degree, *betweenness* and *bridging* centralities. This observation agreed with the significant and non-trivial link we found between the *infomap*-kinless category and this group of genes. Moreover, this result suggested that the *infomap*-participation feature provided the most effective topological alternative, among the considered ones, to bring out this particular gene-set from protein interaction data (in particular, more effective than other information-flow related quantities like node *betweenness* or *bridging* centrality).

#### 4 DISCUSSION

In our analysis of the modular structure of a human PIN, we found that both, CNM and *infomap* clusterization algorithms, produced high-quality network partitions in terms of achieved modularity values. However, significant differences arose in terms of the granularity of each description. In particular we verified that the largest structures detected by CNM were further broken up in smaller clusters according to the *infomap* network modular de-scription, suggesting that the observed discrepancies were rooted in the resolution limit effect [12] that affects the performance of the CNM community recognition procedure.

In concordance with these findings, we observed a general increase in the number of nodes with high-participation roles according to the high-granularity network partition. Internal surfaces might appear within large CNM clusters when the *infomap* partition was considered, causing a number of originally



intra-CNM-cluster links to become edges connecting different infomap clusters. Importantly, the same behavior was observed when already published data was re-analyzed with the infomap prescription (Fig S4). This finding certainly relativized Guimera's original claim that non-hub kinless nodes were not supposed to be found in real-world networks [6]. Instead, we demonstrated that this could eventually arise only as a consequence of the employed community detection methodology, better than reflecting an intrinsic feature of the analyzed network.

Furthermore, in our work we found that the observed discrepancies in the cluster resolution level, had non-trivial counterparts in the biological coherence of the detected network structures (infomap structures presented greater levels of biological coherence), and secondly in the kind of connectivity patterns each algorithm was able to unveil for the analysis of considered protein-set of interest.

Studying topological network features of proteins related to aging we observed that they could be significantly linked to low and mid participation hub-roles according to the CNM partition (Table S2). However, should the infomap partition be taken into consideration, the same gene-set would have been found to be significantly enriched in high-participation roles (kinless and kinless-hub categories) instead. Noteworthy, for neither hub category we could rule out that the observed enrichment could have arisen from the particular degree distribution exhibited by the corresponding network nodes, as degree-aware random samples showed associations of similar statistical significance levels than the originally observed one. Only the non-hub high participation kinless role detected within the infomap description, proved to be non-trivially connected to the aging related gene set. This means that the corresponding association was particularly supported by the displayed inter and intra modular connectivity pattern of the network nodes.

Importantly, these results suggest that being associated to high infomap-participation nodes (i.e. nodes mostly located at infomap-cluster's interfaces), these proteins could serve for coordination and/or information flow purposes between modules of specific biological functionality. A paradigmatic example of an infomap-kinless protein related to aging is sirtuin 1. SIRT1 and other members of the sirtuin family (SIRT3 and SIRT6) contribute to healthy aging in mammals [34]. In particular, the association of SIRT1 with aging has been proposed based on its role in several processes such as genomic stability, metabolic efficiency, mitochondrial biogenesis, proteostasis and inflammatory responses related to aging [34]. The proteins encoded by the CDKN2A gene provide another interesting example of aging related gene-products associated to infomap-kinless nodes. This gene gives rise to several isoforms known to function as inhibitors of CDK4 kinase, such as p16 and p19. The levels of both p16 and p19 are correlated to the chronological age of tissues in humans and animal models. More interestingly, the CDKN2A gene locus was found to be associated to several of age-associated diseases in a meta-analysis of GWAS [35]. Based on these evidences, the CDKN2A gene is regarded as the best documented gene that control human aging and is associated to age-related diseases.

## 5 CONCLUSIONS

In this manuscript we addressed in a systematic manner how alternative modular descriptions of a biological network, displaying different granularity levels, could condition the outcome of follow-up network biology analysis. In particular we analyzed the use of two paradigmatic and well-known community recognition algorithms, namely the *CNM* and *infomap* procedures, and thoroughly characterized their performance in terms of the granularity of the corresponding inferred network partitions and the biological homogeneity displayed by the detected network structures.

We observed that the *infomap* partition resulted in a keener description of the network's modular structure than the *CNM* prescription, and argued that the resolution limit, inherent to modularity based optimization procedures like *CNM*, could lie behind this behavior. To our knowledge, the resolution limit effect has not been evaluated before in the context of biological networks. Noticeably, we found that *infomap* clusters not only corresponded to congruent structures from the topological perspective, but also displayed higher levels of biological homogeneity. Discrepancies in the cluster resolution level displayed by each algorithm had also impinged on the specific kind of meso-scale connectivity patterns each methodology was able to unveil. In this regard, we presented a thoughtful analysis of differences arising in the significant statistical associations that could be established between intra/inter modular connectivity patterns, and specific protein sets related to complex phenotypes like aging.

Overall, our results raises a word of caution regarding the technical tools used in network biology analysis, and suggests that the high granularity modular description provided by the *infomap* procedure outperforms the *CNM* prescription in terms of its ability to detect statistically significant and biologically sensible associations between the considered biologically motivated protein-sets and a cartographic role classification.

## 6 ACKNOWLEDGMENTS

Funding: The research leading to these results received support from CONICET (PIP0087), UBACyT (20020110200314), ISCIH-FEDER (PI13/00082 and CP10/00524), the IMI JU under grants agreements nº [115002] (eTOX) and nº [115191] (Open PHACTS)], resources of which are composed of financial contribution from the EU's FP7 (FP7/2007-2013) and EFPIA companies' in kind contribution. The GRIB is a node of the Spanish National Institute of Bioinformatics (INB).

## 7 REFERENCES

- [1] Barabási A-L, Oltvai ZN (2004) *Network biology: understanding the cell's functional organization*. *Nat Rev Genet* 5: 101–113. doi:10.1038/nrg1272.
- [2] Csermely P, Korcsmáros T, Kiss HJM, London G, Nussinov R (2013) Structure and dynamics of molecular networks: a novel paradigm of drug discovery: a comprehensive review. *Pharmacol Ther* 138: 333–408. doi:10.1016/j.pharmthera.2013.01.016.

- [3] Hartwell LH, Hopfield JJ, Leibler S, Murray AW (1999) From molecular to modular cell biology. *Nature* 402: C47–52. doi:10.1038/35011540.
- [4] Barabási A-L, Gulbahce N, Loscalzo J (2011) Network medicine: a network-based approach to human disease. *Nat Rev Genet* 12: 56–68. doi:10.1038/nrg2918.
- [5] Sunyaev S, Roth F, Carter H, Hofree M, Ideker T (2013) Genotype to phenotype via network analysis. *Curr Opin Genet Dev* 23: 611–621.
- [6] Guimerà R, Amaral LAN (2005) Cartography of complex networks: modules and universal roles. *J Stat Mech Online* 2005: nihpa35573. doi:10.1088/1742-5468/2005/02/P02001.
- [7] Guimerà R, Amaral LAN (2005) Functional cartography of complex metabolic networks. *Nature* 433: 895–900. doi:10.1038/nature03288.
- [8] Guimerà R, Sales-Pardo M, Amaral LAN (2007) Module identification in bipartite and directed networks. *Phys Rev E Stat Nonlin Soft Matter Phys* 76: 036102.
- [9] Fortunato S (2010) Community detection in graphs. *Phys Rep* 486: 75–174. doi:10.1016/j.physrep.2009.11.002.
- [10] Clauset A, Newman M, Moore C (2004) Finding community structure in very large networks. *Phys Rev E* 70: 066111. doi:10.1103/PhysRevE.70.066111.
- [11] Rosvall M, Bergstrom CT (2008) Maps of random walks on complex networks reveal community structure. *Proc Natl Acad Sci U S A* 105: 1118–1123. doi:10.1073/pnas.0706851105.
- [12] Fortunato S, Barthélemy M (2007) Resolution limit in community detection. *Proc Natl Acad Sci U S A* 104: 36–41. doi:10.1073/pnas.0605965104.
- [13] Lancichinetti A, Fortunato S (2009) Community detection algorithms: A comparative analysis. *Phys Rev E* 80: 056117. doi:10.1103/PhysRevE.80.056117.
- [14] Aldecoa R, Marín I (2013) Exploring the limits of community detection strategies in complex networks. *Sci Rep* 3: 2216. doi:10.1038/srep02216.
- [15] Lancichinetti A, Fortunato S (2011) Limits of modularity maximization in community detection. *Phys Rev E* 84: 066122. doi:10.1103/PhysRevE.84.066122.
- [16] Xiang J, Hu XG, Zhang XY, Fan JF, Zeng XL, et al. (2012) Multi-resolution modularity methods and their limitations in community detection. *Eur Phys J B* 85: 352. doi:10.1140/epjb/e2012-30301-2.
- [17] Agarwal S, Deane CM, Porter M a, Jones NS (2010) Revisiting date and party hubs: novel approaches to role assignment in protein interaction networks. *PLoS Comput Biol* 6: e1000817. doi:10.1371/journal.pcbi.1000817.
- [18] Pritykin Y, Singh M (2013) Simple topological features reflect dynamics and modularity in protein interaction networks. *PLoS Comput Biol* 9: e1003243. doi:10.1371/journal.pcbi.1003243.
- [19] Chang X, Xu T, Li Y, Wang K (2013) Dynamic modular architecture of protein-protein interaction networks beyond the dichotomy of “date” and “party” hubs. *Sci Rep* 3: 1691. doi:10.1038/srep01691.

- [20] Schaefer MH, Fontaine J-F, Vinayagam A, Porras P, Wanker EE, et al. (2012) HIPPIE: Integrating protein interaction networks with experiment based quality scores. *PLoS One* 7: e31826. doi:10.1371/journal.pone.0031826.
- [21] De Magalhães JP, Budovsky A, Lehmann G, Costa J, Li Y, et al. (2009) The Human Ageing Genomic Resources: online databases and tools for biogerontologists. *Aging Cell* 8: 65–72. doi:10.1111/j.1474-9726.2008.00442.x.
- [22] Erdős P, Rényi A (1959) On random graphs, I. *Publ Math* 6: 290–297.
- [23] Viger F, Latapy M (2005) Efficient and Simple Generation of Random Simple Connected Graphs with Prescribed Degree Sequence. In: Wang L, editor. *Computing and Combinatorics SE - 45. Lecture Notes in Computer Science*. Springer Berlin Heidelberg, Vol. 3595. pp. 440–449. doi:10.1007/11533719\_45.
- [24] Team RC (2013) A Language and Environment for Statistical Computing.
- [25] Csardi G, Nepusz T (2006) The igraph software package for complex network research. *InterJournal Complex Sy*: 1695.
- [26] Datta S, Datta S (2006) Methods for evaluating clustering algorithms for gene expression data using a reference set of functional classes. *BMC Bioinformatics* 7: 397. doi:10.1186/1471-2105-7-397.
- [27] Antebi A (2007) Genetics of aging in *Caenorhabditis elegans*. *PLoS Genet* 3: 1565–1571. doi:10.1371/journal.pgen.0030129.
- [28] Witten TM, Bonchev D (2007) Predicting aging/longevity-related genes in the nematode *Caenorhabditis elegans*. *Chem Biodivers* 4: 2639–2655. doi:10.1002/cbdv.200790216.
- [29] Lu T, Pan Y, Kao S-Y, Li C, Kohane I, et al. (2004) Gene regulation and DNA damage in the ageing human brain. *Nature* 429: 883–891. doi:10.1038/nature02661.
- [30] Boyd-Kirkup JD, Green CD, Wu G, Wang D, Han J-DJ (2013) Epigenomics and the regulation of aging. *Epigenomics* 5: 205–227. doi:10.2217/epi.13.5.
- [31] Xue H, Xian B, Dong D, Xia K, Zhu S, et al. (2007) A modular network model of aging. *Mol Syst Biol* 3: 147. doi:10.1038/msb4100189.
- [32] West J, Widschwendter M, Teschendorff AE (2013) Distinctive topology of age-associated epigenetic drift in the human interactome. *Proc Natl Acad Sci U S A* 110: 14138–14143. doi:10.1073/pnas.1307242110.
- [33] Hwang W, Cho Y, Zhang A, Ramanathan M (2006) Bridging Centrality: Identifying Bridging Nodes in Scale-free Networks. *Dep Comput Sci Eng Univ Buffalo Technical*.
- [34] López-Otín C, Blasco MA, Partridge L, Serrano M, Kroemer G (2013) The hallmarks of aging. *Cell* 153: 1194–1217. doi:10.1016/j.cell.2013.05.039.
- [35] Jeck WR, Siebold AP, Sharpless NE (2012) Review: a meta-analysis of GWAS and age-associated diseases. *Aging Cell* 11: 727–731. doi:10.1111/j.1474-9726.2012.00871.x.

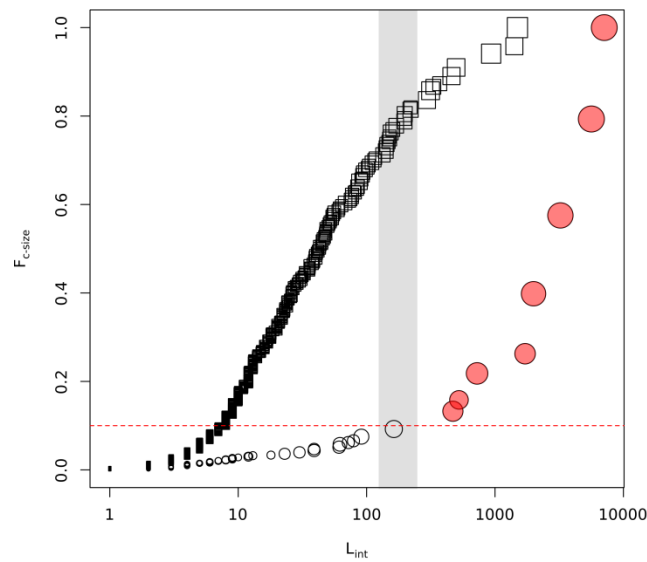


**Fig 1** Analysis of cluster partitions obtained with *CNM* (circles) and *infomap* (empty squares) methodologies. The panel shows the cumulative cluster-size function as a function of  $l_{int}$ . Symbol sizes were set using a scale proportional to the log-size of the corresponding cluster. The horizontal line corresponds to the 10% accumulated mass level. Dashed vertical lines delimit a region of values of the order square root of total number of links in the network,  $[\sqrt{L/2}, \sqrt{2L}]$ , corresponding to the natural scale found to operate in modularity optimization procedures [Fortunato2007, Lancichinetti2011].

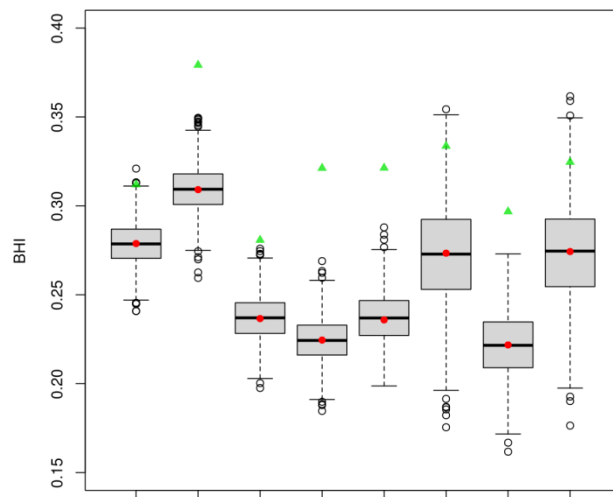


**Fig 2** The Biological Homogeneity Index,  $BHI$ , estimated for each of the 8 CNM largest communities, is depicted as red points (CNM clusters are ordered according decreasing size). Green triangles show the  $BHI$  level of the *infomap* partition of clusters included in the respective *CNM* structure. For each CNM community, boxplots depict main features of  $BHI$  distributions estimated for an ensemble of 1000 random shuffling realizations of the corresponding *infomap* labels. Noticeably, the mean  $BHI$  values of the randomized partitions agree with the  $BHI$  level obtained for the corresponding structure-less CNM clusters (red points)

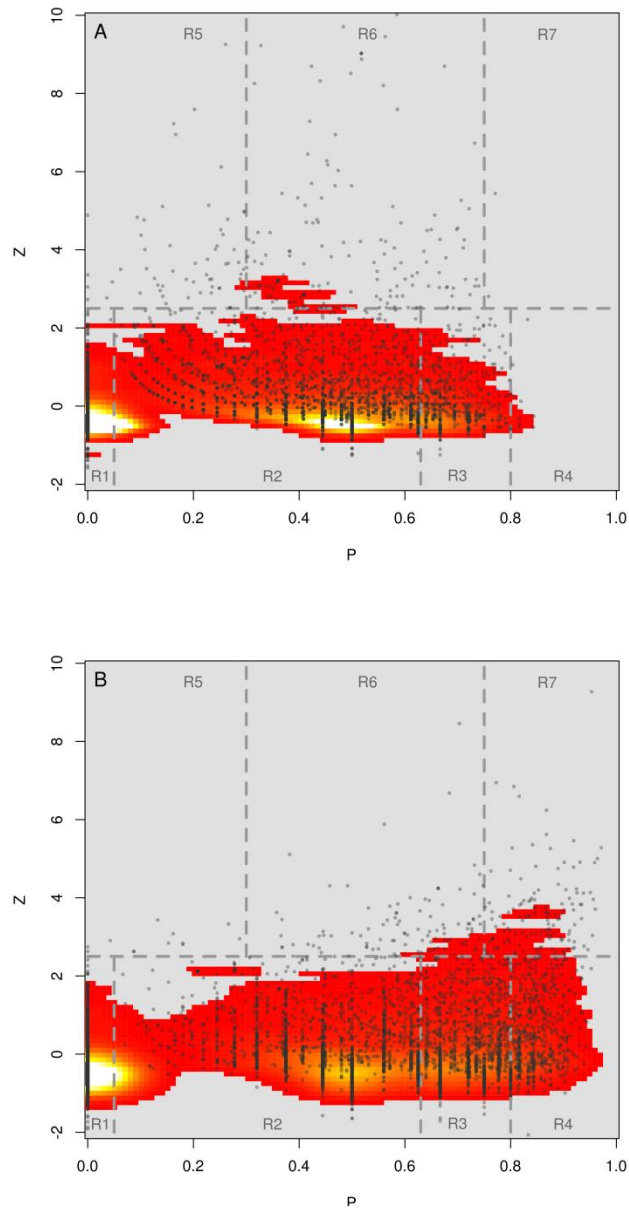


**Fig 3** Distributions of *PIN* nodes in the *Z-P* plane obtained when the *CNM* and *infomap* clusterization were considered are shown in top and bottom panels respectively. A color-coded kernel density estimation was also depicted in the figures. Dashed lines in the figure delineate regions corresponding to the seven different universal roles [6]

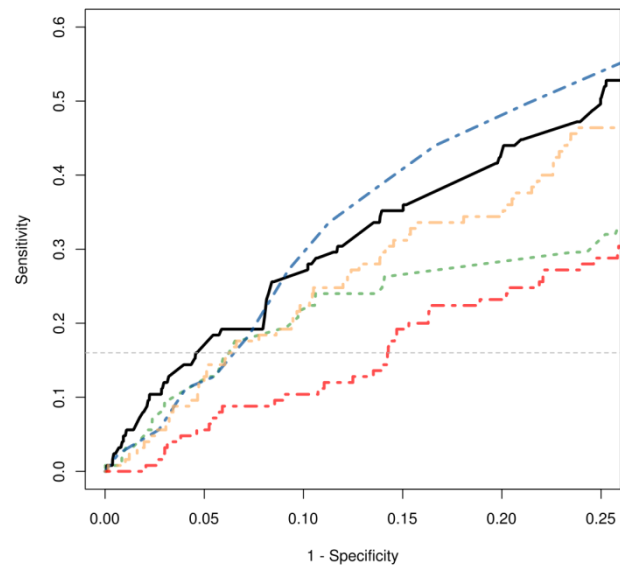


**Fig 4** - ROC curves for ARG genes based on node's *infomap*-participation, *CNM*-participation, degree, bridge-centrality and betweenness feature levels are shown as solid black, orange dashed, blue dotted-dashed, dotted-dashed red and green dashed lines respectively. Only nodes with mid/low connectivities (i.e. network nodes with degree values lower than the 90% percentile of the entire degree distribution) were considered. The horizontal dotted line depicts the maximum sensitivity level achieved *infomap*-kinless ARG gene with the lowest *infomap*-participation value



# SUPPLEMENTARY MATERIAL

## Mining the modular structure of protein interaction networks at different resolution levels

Berenstein A.\*<sup>1</sup>, Piñero J.\*<sup>2</sup>, Furlong L.<sup>2</sup>, Chernomoretz A.<sup>1,3</sup>

### *ST1 - Protein interaction network characterization*

We began our analysis summarizing main general topological features related to the *degree* distribution, *clustering coefficient*[1], and *betweenness*[2] of the nodes of the considered HN. These quantities assess for the number of neighbors, the connectivity among them, and the node relevance in terms of global information flux over the entire network, respectively.

A network characterization in terms of node degree distribution involved one of the most basic and intuitive connectivity-related notion of centrality. The protein interaction network exhibited a heavy-tailed empirical degree distribution - gray points in Figure S1 - reflecting large fluctuations in vertex connectivity (while the network nodes presented an average degree of  $\bar{k} = 7.7$ , the maximum degree was  $k_{max}=492$ ). This feature is not recapitulated in the ERN null model (see the Method section for a brief description of the considered network null models) - yellow points in Figure S1a - for which the existence of a natural scale for vertex connectivity can be recognized. This fundamental discrepancy has already been widely reported for many different real world networks, and highlights the existence of non-trivial correlation patterns at the level of vertices connectivity.

The heterogeneity observed in neighbor numbers implies the existence of unusually highly connected hub nodes that could act as general shortcuts, globally shortening geodesic distances over the entire network. However, in terms of global information spreading capabilities, additional non-trivial relevant network nodes might also exist. The *betweenness* centrality concept aims to exploit this information-flux point of view to characterize structural properties of network nodes. Figure (S1b) displays the node's *betweenness* as a function of the node's degree for HN, ERN, and RWN (shown as gray, yellow and red circles respectively). A monotonic and increasing relationship can be recognized for all the three considered networks, denoting the somehow expected general positive correlation trend that exists between the degree and betweenness of a node. Noticeably, for a given degree value, the bio-molecular network presented a wider distribution of betweenness levels. In addition, it presented a higher fraction of high-betweenness and low-degree nodes than the two alternative random network models. If only low connectivity vertices (e.g. having less  $\bar{k} = 7.7$  neighbors) were considered, forty nine nodes would be found within the top-10% betweenness score ranking in HN, while four and none in the RWN and ERN cases respectively. These *bottleneck* nodes, that are overrepresented in the real network, constitute an *a priori* interesting subset of proteins since they could play a

central intermediary role in information transmission processes taking place over the entire network [2,3] .

Insights about local connectivity patterns can also be gained looking at the node's *clustering coefficient* that quantifies the connectivity among first neighbors of a given node. Figure (S1c) displays the *clustering coefficient* as a function of the node's degree for HN, ERN, and RWN (shown as gray, yellow and red circles respectively). An expected general negative correlation trend can be observed between these two quantities for the three networks. However a much larger number of nodes presenting high clustering coefficient values can be observed for HN.

The presented results suggested the existence of non-trivial topological heterogeneities compatible with a putative underlying modular organization in HN, our bio-molecular network of interest, similarly to what have already been reported in other biological inspired network-based analysis [4-6]. Moreover, the observed structural differences with respect to randomized networks allow us to anticipate that HN interconnectivity patterns probed by different topological observables could highlight non-trivial network components, such us high-betweenness, low-connectivity proteins that might act as important links between modular structures.

## *ST2 - Clustering procedures*

The *CNM* algorithm looks for communities by direct optimization of the modularity  $Q$  of the graph, that is defined, up to a multiplicative constant, as the number of edges falling within groups minus the expected number in an equivalent network with edges placed at random:

$$Q = \frac{1}{2L} \sum_{ij}^N \left( A_{ij} - \frac{k_i k_j}{2L} \right) \delta(C_i, C_j) \quad [1]$$

In the above equation,  $k_i$  is the degree of node- $i$ ,  $L$  is the total number of network edges,  $N$  the total number of nodes,  $A_{ij}$  is the adjacency matrix of the network ( $A_{ij}=1$  if there is a link between nodes  $i$  and  $j$ , and zero otherwise).  $C_i$  identifies the cluster that includes node- $i$ , and  $\delta(C_i, C_j)$  is a delta function (i.e.  $\delta(C_i, C_j) = 1$  if node- $i$  and node- $j$  belong to the same cluster, and zero otherwise).

On the other hand, the *infomap* algorithm relies on very different optimization criteria. Clusters are defined in order to minimize the average description length of random walk process taking place over the graph. A two level hierarchy, involving a community tag and a within-community ID tag, is used to identify each network node. As random walkers are expected to expend a lot of time inside densely structures in the graph (i.e. communities), the algorithm iteratively search for node-tagging schemes that produce increasingly compact descriptions of the random walk process. As a by product, a sensible description of the network modular structure is achieved. The *infomap* objective function can be thought in terms of the entropy associated to the random walk process and involved two contribution terms. The first one represents the entropy of the movement between modules, while the second one corresponds to movements within modules:

$$L(P) = q_{inter}H(Q) + \sum_i^s p_{intra}^i H(P^i) \quad [2]$$

Here,  $q_{inter}$  is the probability that the walker switches clusters,  $H(Q)$  is the entropy associated to between clusters transitions,  $p_{intra}^i$  is the fraction of movements occurring inside cluster  $i$ , and  $H(P^i)$  is the entropy of movements within the cluster  $i$ . [7].

As can be seen from equations (1) and (2) both considered algorithms rely on very different assumptions and optimization criteria, and thus could provide in principle alternative and complementary descriptions of the modular structure of the analyzed network. A more detailed and general description of optimization criteria and performance comparison of both algorithms can be found in [8,9].

### *ST3 – BHI*

Following Datta&Datta[10], we considered a partition of  $k$  clusters,  $\{D_1, D_2, \dots, D_k\}$ , and assumed that  $C(x)$  is a functional class containing gene  $x$ . The biological homogeneity index of the partition resulted:

$$BHI = \frac{1}{k} \sum_{j=1}^k \frac{1}{n_j(n_j - 1)} \sum_{x \neq y \in D_j} I(C(x) = C(y))$$

where  $n_j$  is the size of cluster- $j$ . The indicator function  $I(C(x) = C(y))$  takes the value 1 if  $C(x)$  and  $C(y)$  match. We made use of the functionality implemented in the *clValid* R-package[11], and disregarded functional GO classes annotated under the IEA (inferred from electronic annotations) evidence code.

### *ST4-Bootstrap with degree control*

A bootstrapping procedure was devised for the topographic role enrichment analysis of the considered gene-groups in order to control for the node's degree distribution factor. For each enrichment test, we considered an ensemble of 1000 control random gene-sets having the same degree distribution than genes under study, and a p-value level was estimated according to the number of random realizations displaying the same or larger effects (over/under representation significance) than the ones observed in the original data.

Each random realization was conformed according the degree displayed by the original gene set randomly extracting genes from pools of given degree levels. In order to warrant for a non-biased sampling, we binned by degree the available sampling nodes requiring a minimal sample size of 100 nodes per bin. Once the non-uniform binning was established we made an *a-posteriori* analysis to make sure that the degree distributions of control random realizations had similar statistical features than the observed one. To that end, we identified which quantile level of the original data was not duly sampled looking for cases where the corresponding observed

degree were not included in the inter-quartile range of the respective control realizations. For instance, it can be appreciated from figure S7 that the high degree level of the top 10% of the ARG set, could not be reproduced by the random sampling procedure. In this case the bootstrap analysis was performed considering a reduced ARG' set, discarding the 10% most connected aging related genes.

### *ST5 -Participation-based analysis of alternative PPI networks*

In this section we considered two PPI-Yeast Networks recently analyzed by Chang et al. [12] to investigate the party-date hub dichotomy using the Z-P topological features.

We first considered a high confidence yeast PIN introduced and curated by Batada[13]. Its giant component presented 3801 nodes, and 9742 links. The second considered Yeast PIN was originally proposed by Bertin [14]. Its giant component presented 2233 nodes and 5750 links.

The modular structure of these networks was analyzed using both, the CNM and infomap community detection algorithms. The corresponding Z-P density distributions are shown in (fig.S4). It can be observed that high participation nodes are precluded according to the CNM low-resolution description. On the other hand, the use of the infomap clustering procedure resulted in a noticeable increase of this type of nodes.

		<i>CNM</i>							
<i>Infomap</i>		<i>R1</i>	<i>R2</i>	<i>R3</i>	<i>R4</i>	<i>R5</i>	<i>R6</i>	<i>R7</i>	<i>Total</i>
	<i>R1</i>	3009	152	1	0	0	0	0	3162
	<i>R2</i>	716	1497	84	0	18	32	0	2347
	<i>R3</i>	146	936	500	0	7	21	0	1610
	<i>R4</i>	9	304	288	11	4	19	0	635
	<i>R5</i>	3	6	0	0	3	0	0	12
	<i>R6</i>	1	44	5	0	18	34	0	102
	<i>R7</i>	0	25	31	2	8	64	2	132
	<i>Total</i>	3884	2964	909	13	58	170	2	8000

**Sup Table 1.** Distribution of cartographic role assignments according to the Infomap and CNM descriptions. Cartographic role abbreviation: Ultra peripheral (R1), Peripheral (R2), Connector (R3), Kinless (R4), Provincial Hubs (R5), Connector Hubs (R6), Kinless Hubs (R7). The coarser resolution level achieved by the *CNM* algorithm resulted in a general tendency to assign lower participation coefficient values to network nodes. For instance 68% of *infomap*-connector vertices were assigned to lower participation roles (59% peripheral, 9% ultra-peripheral) when the CNM procedure was considered. More strikingly, the majority (94%) of the 635 *infomap*-kinless nodes were re-classified as: CNM-connectors (45%), CNM-peripheral (48%), and CNM-ultra-peripheral nodes (1%). Finally, it can also be observed that nodes originally assigned to hub-like roles when *infomap* procedure was employed were not only affected by this lowering effect in the participation, but in addition, almost 50% of them were also reassigned to non-hub roles when CNM was considered

		<i>Cartography</i>		<i>ARG dataset</i>		<i>ARG' dataset</i>		
		<i>Role</i>	<i>N</i>	<i>ARG</i>	<i>pv</i>	<i>ARG'</i>	<i>pv</i>	<i>pv'</i>
<i>CNM</i>	<i>Non Hubs</i>	<b>R1</b>	3884	47	1	47	1	1
		<b>R2</b>	2964	119	0.00989	119	4.60E-05	0.488
		<b>R3</b>	909	47	0.00413	46	0.000382	0.121
		<b>R4</b>	13	1	1	1	0.447	0.111
	<i>Hubs</i>	<b>R5</b>	58	15	<b>1.72E-09</b>	8	0.000584	0.417
		<b>R6</b>	170	32	<b>2.19E-15</b>	12	0.00693	0.998
		<b>R7</b>	2	0	1	0	1	1
<i>Infomap</i>	<i>Non Hubs</i>	<b>R1</b>	3162	26	1	26	1	1
		<b>R2</b>	2347	51	1	51	1.00E+00	1
		<b>R3</b>	1610	65	0.13	65	0.0558	0.286
		<b>R4</b>	635	67	<b>4.95E-18</b>	67	<b>6.67E-21</b>	0
	<i>Hubs</i>	<b>R5</b>	12	1	9.86E-01	1	0.418	0.622
		<b>R6</b>	102	11	2.32E-03	7	5.07E-02	0.98
		<b>R7</b>	132	40	<b>1.00E-27</b>	16	<b>4.37E-06</b>	0.352

**Table 2.**Summary of Fisher statistical association test between the ARG set and cartographic role assignments.

Summary of Fisher statistical association test between the ARG set and cartographic role assignments considering the *CNM* (first 7 rows) and *infomap* (last 7 rows) modular descriptions are shown in the first 4 columns. Results of the corresponding bootstrap control tests are shown in the last three table columns. The number of network's nodes, ARG nodes, and ARG' nodes, assigned to a given role are displayed in columns: *N*, *ARG*, and *ARG'* respectively. Fdr-adjusted Fisher enrichment p-values are reported in **ARG-*pv*** and **ARG'-*pv*** columns, where fdr-adjusted bootstrap p-values (see Methods) are shown in column *pv'*. Cartographic role abbreviation: Ultra peripheral (R1), Peripheral (R2), Connector (R3), Kinless (R4), Provincial Hubs (R5), Connector Hubs (R6), Kinless Hubs (R7).

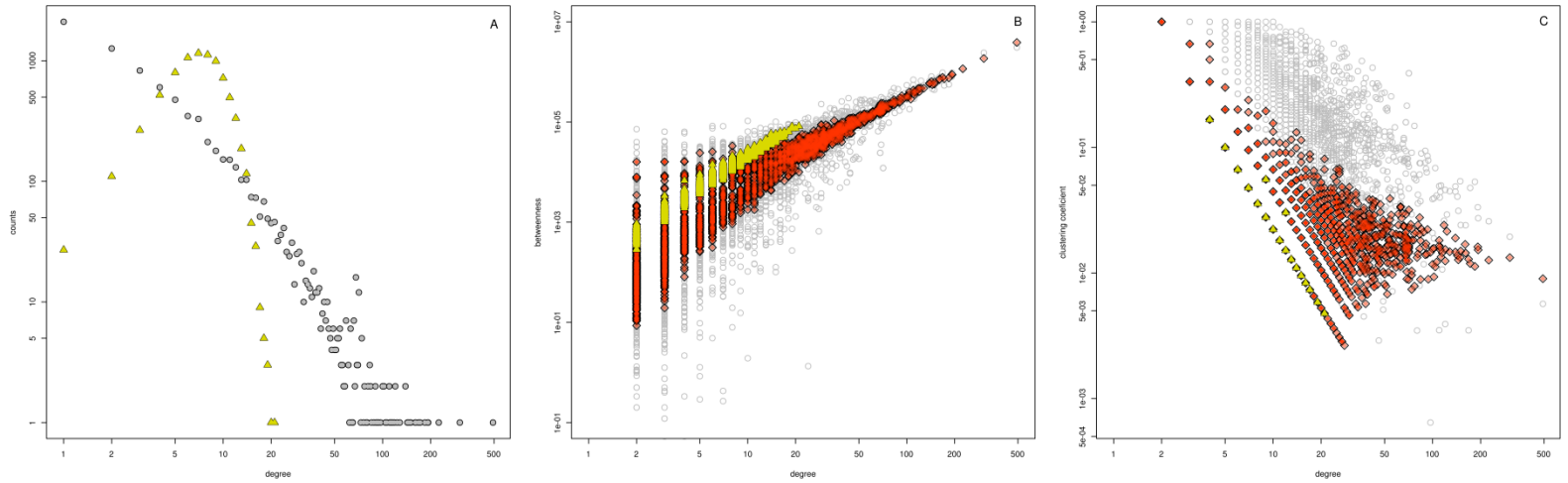


Figure S1 - Topological features of HIPPIE network. (A) node degree distribution for HIPPIE network (gray circles), and for the respective Erdos-Renyi random network (yellow triangles). Nodes of the HIPPIE network (gray circles), Rewired Network (red diamonds) and Erdos-Renyi network (yellow triangles) were displayed over the Degree-Betweenness and the Degree-Clustering Coefficient planes in panels (B) and (C) respectively.

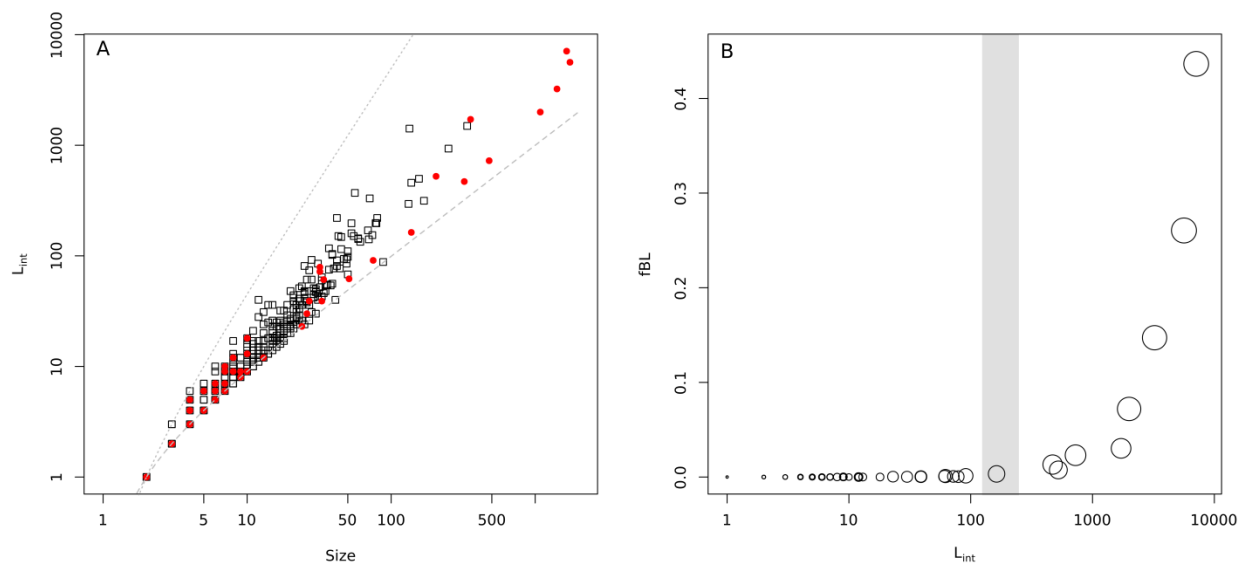


Fig S2 . (a) Number of internal links,  $L_{int}$ , as a function of cluster sizes. The dotted and dashed lines depict the expected relationships for fully connected cliques and linear structures respectively, and are included for reference purposes. (b) Fraction of internal CNM cluster's links that did not appear as internal links in the infomap modular description (i.e. fraction of broken links, fBL). Circles represent CNM clusters and their radius are proportional to each cluster log-size.



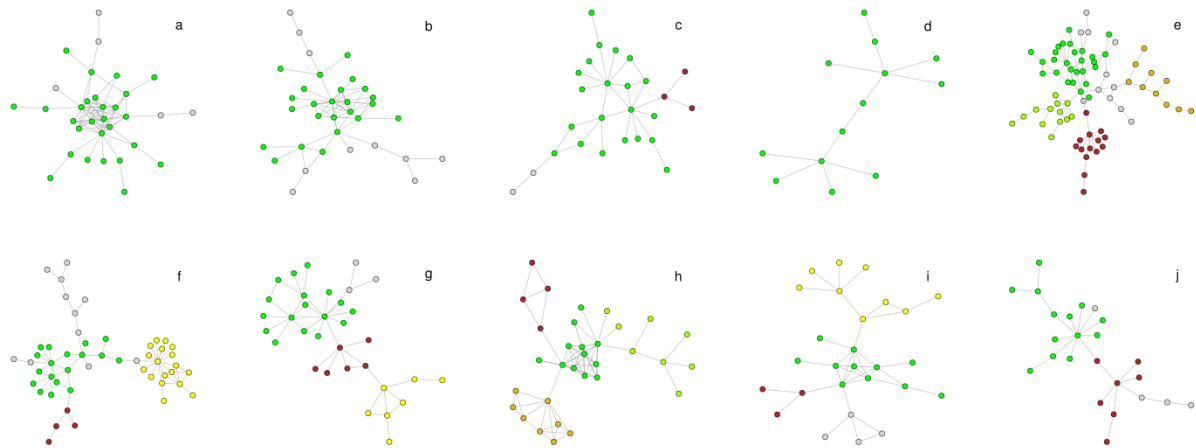


Fig S3 *CNM* clusters with low internal-link density and more than ten nodes. *infomap* communities were depicted using different colors. Gray colored nodes belonged to infomap clusters not-totally included in the displayed *CNM* structure. Two scenarios can be recognized. For cases (a)-(d) a rather good agreement between the alternative modular descriptions was observed. On the contrary, for the cases illustrated in panels (e)-(j) internal structure not resolved by the *CNM* procedure was indeed highlighted by the infomap prescription.

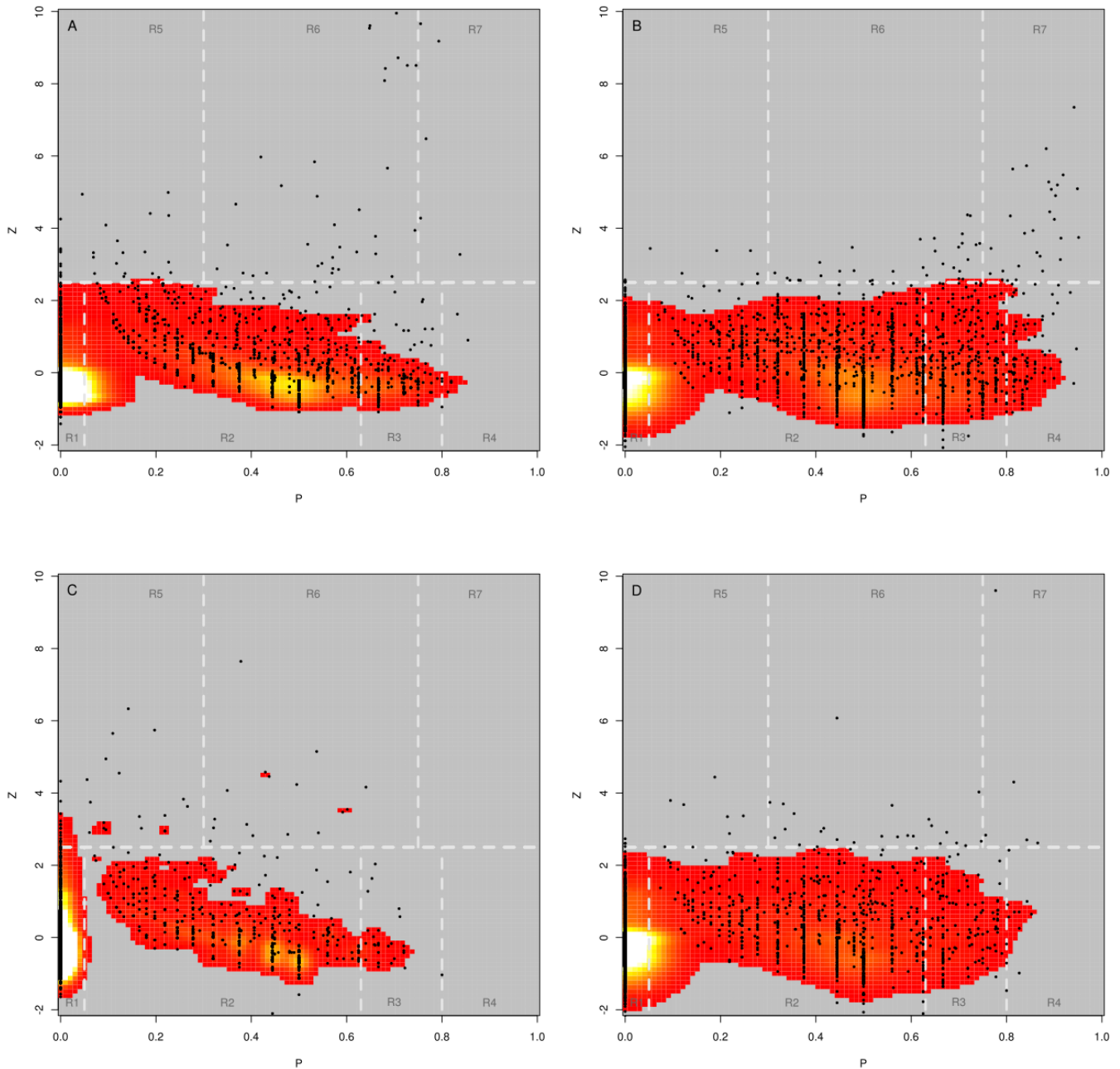
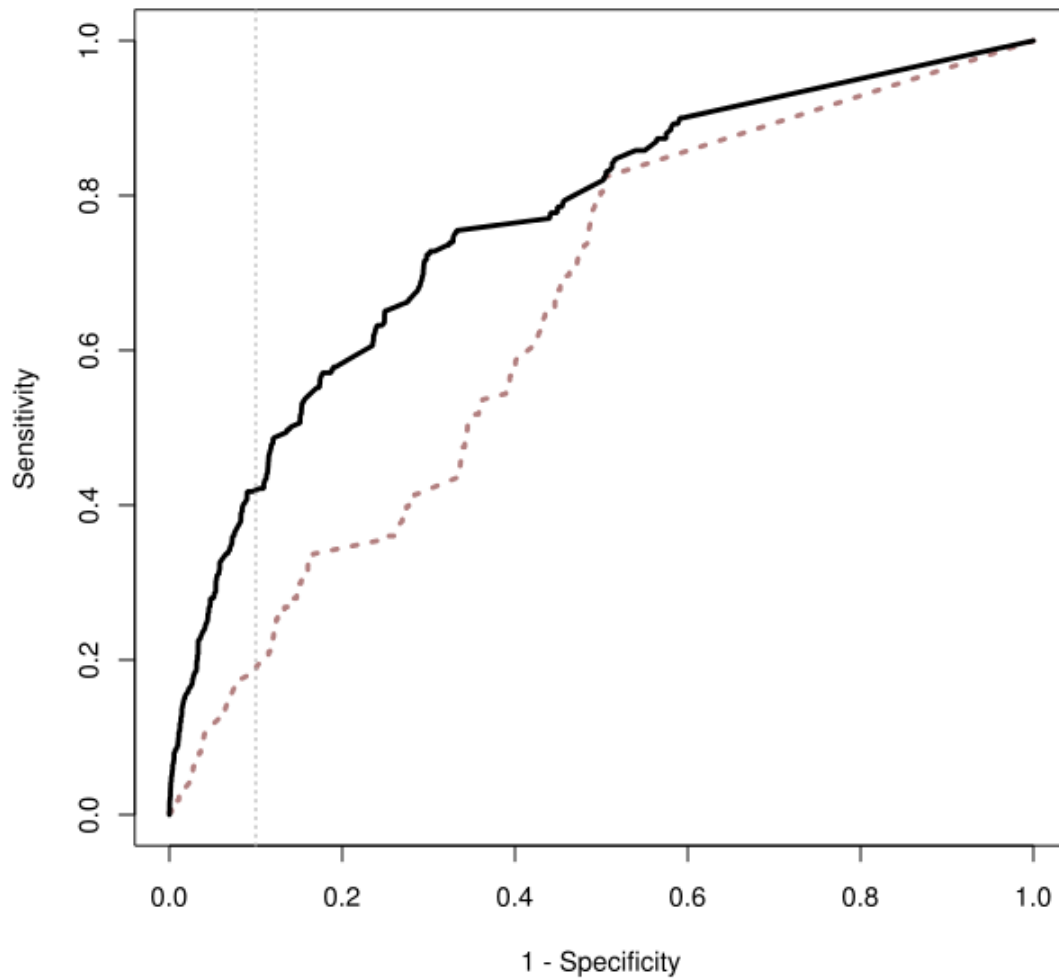


Figure S4 - Z-P planes for Batada yeast PPI network (panels A-B) and Bertinyeast PPI Network (panels C-D). Left and right panels correspond to *CNM*-based and *infomap*-based cartographical descriptions respectively. An overall increasing behavior in node participation levels can be observed when the *infomap* cluster recognition procedure was considered.



FigureS5 -Participation-based ROC curves estimated for ARG genes for *CNM* and *infomap* modular descriptions are shown with dashed brown and continuous black lines respectively. The vertical dotted line represents the 90% specificity level. Statistically significant differences between total AUCs are observed (AUC-IFM =0.76; AUC-CNM=0.65;  $p$ value<e-16, deLong's test), suggesting that the resolution level provided by *infomap* enhanced the detection of the topological bias displayed by ARG genestoward high-participation levels.

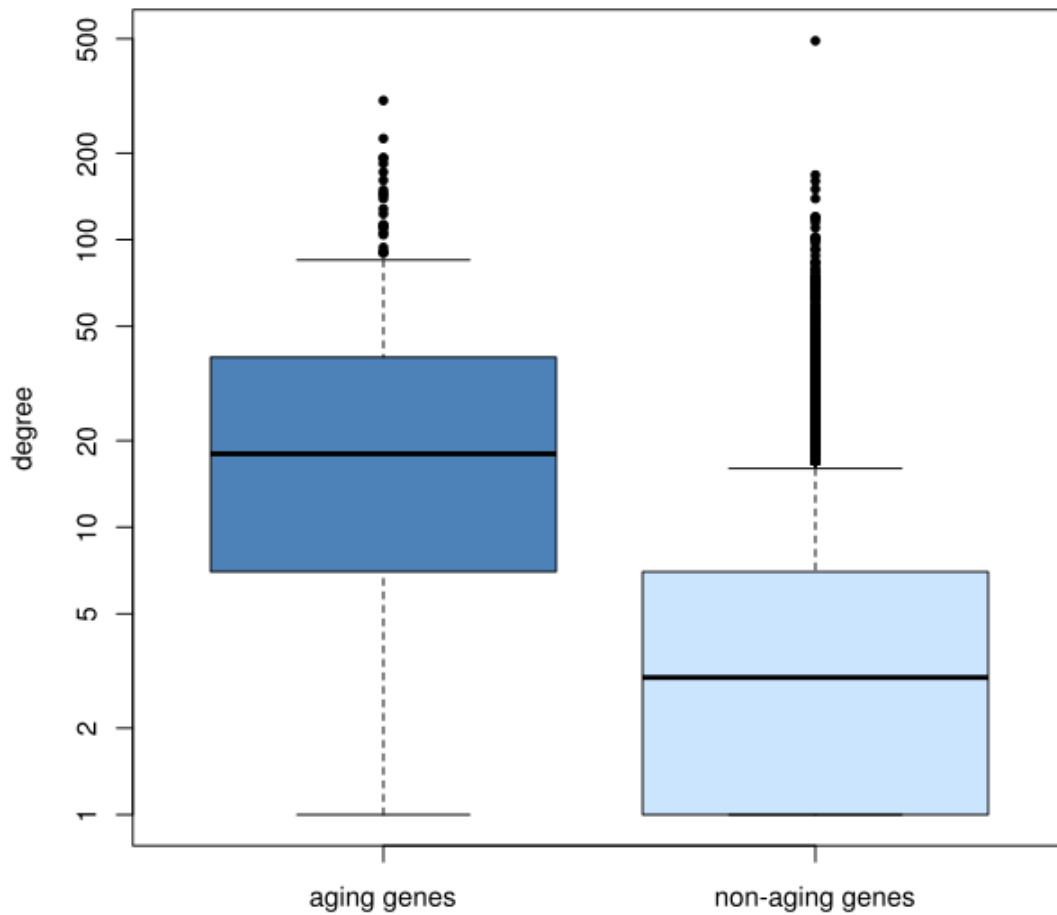


Figure S6 - The degree distribution of aging genes, and the whole HIPPIE network remaining nodes are shown in the left and right boxplots respectively. Significant differences ( $p < e-16$ , Wilcoxon test) were observed between both degree distributions.

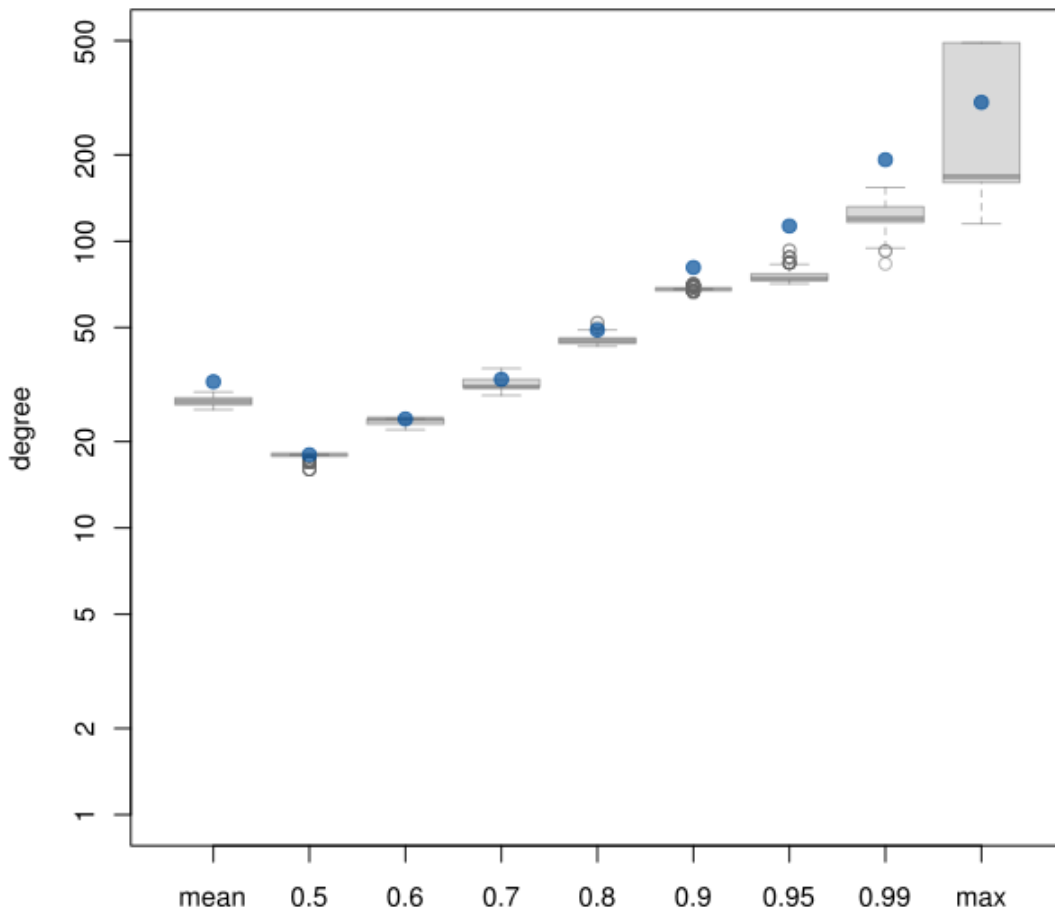


Figure S7- Degree distributions for selected quantiles of 1000 control random realizations are displayed as boxplot. Blue circles depict ARG degree values for the respective quantiles. It can be observed that the top-10% of ARG with highest degree levels, lay outside the inter-quartile levels of their corresponding control random samples.

1. Watts DJ, Strogatz SH (1998) Collective dynamics of “small-world” networks. *Nature* 393: 440–442. doi:10.1038/30918.
2. Freeman L (1977) A Set of Measures of Centrality Based on Betweenness. *Sociometry* 40: 35 – 41.
3. Yu H, Kim PM, Sprecher E, Trifonov V, Gerstein M (2007) The Importance of Bottlenecks in Protein Networks: Correlation with Gene Essentiality and Expression Dynamics. *PLoSComputBiol* 3(4): e59. doi:10.1371/journal.pcbi.0030059
4. Barabási A-L, Oltvai ZN (2004) Network biology: understanding the cell’s functional organization. *Nat Rev Genet* 5: 101–113. doi:10.1038/nrg1272.
5. Guimerà R, Sales-Pardo M, Amaral LAN (2007) Module identification in bipartite and directed networks. *Phys Rev E Stat Nonlin Soft Matter Phys* 76: 036102.
6. Cai JJ, Borenstein E, Petrov DA (2010) Broker Genes in Human Disease. *Genome BiolEvol* 2815–825
7. Rosvall M, Bergstrom CT (2008) Maps of random walks on complex networks reveal community structure. *Proc Natl Acad Sci U S A* 105: 1118–1123. doi:10.1073/pnas.0706851105.
8. Lancichinetti A, Fortunato S (2009) Community detection algorithms: A comparative analysis. *Phys Rev E* 80: 056117. doi:10.1103/PhysRevE.80.056117.
9. Lancichinetti A, Fortunato S (2011) Limits of modularity maximization in community detection. *Phys Rev E* 84: 066122. doi:10.1103/PhysRevE.84.066122.
10. Datta S, Datta S (2006) Methods for evaluating clustering algorithms for gene expression data using a reference set of functional classes. *BMC Bioinformatics* 7: 397. doi:10.1186/1471-2105-7-397.
11. Brock G, Pihur V, Datta S, Datta S (2008) cIValid: An R Package for Cluster Validation. *J Stat Softw* 25: 1–22.
12. Chang X, Xu T, Li Y, Wang K (2013) Dynamic modular architecture of protein-protein interaction networks beyond the dichotomy of “date” and “party” hubs. *Sci Rep* 3: 1691. doi:10.1038/srep01691.
13. Batada NN, Hurst LD, Tyers M (2006) Evolutionary and physiological importance of hub proteins. *PLoS Comput Biol* 2: e88. doi:10.1371/journal.pcbi.0020088.
14. Bertin N, Simonis N, Dupuy D, Cusick ME, Han J-DJ, et al. (2007) Confirmation of Organized Modularity in the Yeast Interactome. *PLoS Biol* 5(6): e153. doi:10.1371/journal.pbio.0050153

